

Kubo-Anderson theory of polariton line shapeClàudia Climent^{1,*}, Joseph E. Subotnik,¹ and Abraham Nitzan^{1,2}¹*Department of Chemistry, University of Pennsylvania, Philadelphia, Pennsylvania 19104, USA*²*School of Chemistry, Tel Aviv University, Tel Aviv 69978, Israel* (Received 24 October 2023; revised 26 January 2024; accepted 22 March 2024; published 8 May 2024)

We apply the Kubo-Anderson stochastic theory of molecular spectral line shapes to the case of polaritons formed in the collective strong-coupling regime. We investigate both the fast and slow limits of the random frequency modulation of the emitter as well as the intermediate regime and show how the interplay between the characteristic timescales of the cavity and the molecular disorder is expressed in the observed polaritons line shapes. The analytical solution obtained for the slow limit is valid for any ratio between the inhomogeneous broadening of the molecules and the Rabi splitting, which is especially relevant for molecular polaritons where these two quantities can be of the same order of magnitude.

DOI: [10.1103/PhysRevA.109.052809](https://doi.org/10.1103/PhysRevA.109.052809)**I. INTRODUCTION**

When the interaction between a photon and an electronic or vibrational transition is strong enough that their rate of energy exchange exceeds that of their respective losses, new hybrid light-matter states known as polaritons are formed [1]. One of the most interesting features of this strong light-matter coupling regime is the collective interaction of an ensemble of emitters with the electromagnetic field in optical cavities. Spectroscopically, this collectivity translates into an energetic (Rabi) splitting between the two polariton modes that scales with the square root of the number of emitters [2]. This collective response and the concept of a polariton as a coherent superposition of states with many different excited molecules naturally raises a question about the possible role of disorder. An interesting spectroscopic as well as numerical observation is that, in the presence of static disorder and for a sufficiently large Rabi splitting, the polariton linewidth does not inherit the inhomogeneous broadening of the cavity-free emitters [3–6]. Instead, the polariton broadening is exclusively due to the homogeneous linewidth of both of its constituents, the cavity and emitter resonances.

Several works have investigated this subject and closely related matters in the past, mostly within the context of semiconductor microcavities [4,5,7–20]. Typically, numerical simulations were carried out to investigate the effect of static disorder on the polariton linewidth, while the effect of (fast) dynamic disorder, which is responsible for the homogeneous broadening, is usually treated phenomenologically. Despite recent interest in the role of disorder in polaritonic phenomena [21–47], especially within the context of molecular polaritons (in which molecular transition bands are quite broad in comparison to atomic systems or semiconductors), an analytic theory capable of describing the effect of both static and dynamic disorders in the polariton line shape is

missing. We address this point by extending the Kubo-Anderson theory of a stochastic molecular line shape [48–53] to the case of many molecules that respond collectively to an optical excitation and, via the same collective response, form polaritons when interacting with resonance cavity modes. Typically, within Kubo theory, the fast and slow limits of frequency fluctuations are characterized as the limits of a unitless modulation parameter $\alpha \equiv \tau_c \Omega$ [53] (see below), which reflects the competition between two timescales: the timescale for frequency modulations τ_c and the inverse magnitude of the amplitude of these frequency modulations $1/\Omega$. Our present extension of the theory to the N -molecule case requires that we account for an important third timescale: the inverse of the Rabi splitting $1/\Omega_R$, which encompasses both the molecule-cavity-mode coupling strength and the collective response of the molecular system. Our theory yields simple analytical results in the slow and fast limits of the disorder dynamics and can be evaluated numerically for the intermediate case. The line-shape expression we obtain for the slow limit is valid for any ratio between the inhomogeneous broadening of the molecules and the Rabi splitting Ω/Ω_R , which is especially relevant for molecular polaritons, in which the broadening due to static disorder can be a significant fraction of the Rabi splitting.

A. Kubo-Anderson theory of stochastic molecular line shape

The starting point of the Kubo-Anderson theory of stochastic line shape is to model a molecular transition as a classical harmonic oscillator whose frequency randomly fluctuates about a central frequency ω_0 due to the interaction with a thermal environment [53]. The dynamics of such an oscillator is described by the following equation of motion:

$$\dot{a} = -i[\omega_0 + \delta\omega(t)]a. \quad (1)$$

The main assumption of the model is that the stochastic time-dependent frequency fluctuation $\delta\omega(t)$ caused by environmental motions is a random stationary Gaussian

*ccliment@sas.upenn.edu

process characterized by an average $\langle \delta\omega(t) \rangle = 0$ and an autocorrelation function for which a common model is $\langle \delta\omega(t)\delta\omega(t+\tau) \rangle = \Omega^2 e^{-\tau/\tau_c}$ with a correlation time $\tau_c = \frac{1}{\Omega^2} \int_0^\infty d\tau \langle \delta\omega(t)\delta\omega(t+\tau) \rangle$, where $\Omega = \sqrt{\langle \delta\omega^2 \rangle}$ is the amplitude of the random frequency modulations. The line shape may then be obtained by calculating the Fourier transform of the autocorrelation function of the amplitude a , $I(\omega) = \int_{-\infty}^\infty dt e^{-i\omega t} \langle a^*(0)a(t) \rangle$, and different physical behaviors are encountered depending on the relative magnitude of the correlation time τ_c and the amplitude of the frequency modulations Ω . Analytical solutions can be obtained in two extreme limits characterized by the magnitude of the dimensionless parameter $\alpha \equiv \tau_c \Omega$.

(1) $\alpha \ll 1$ represents the fast limit, that is, the situation where the dynamics of the environment is fast relative to that of the oscillator. A Lorentzian line shape $I(\omega) = \frac{2\Gamma}{\omega^2 + \Gamma^2}$ is obtained in this limit with a half width at half maximum $\Gamma = \tau_c \Omega^2 = \alpha \Omega$ that can be much narrower than the amplitude of the frequency modulation, a phenomenon known as motional narrowing that has been extensively investigated in NMR spectroscopy [54–56]. Note that the fast limit of the Kubo-Anderson theory is equivalent to the Markovian Bloch-Redfield theory, where it becomes clear that the intrinsic relaxation of the system (with contributions from both population relaxation and pure dephasing) is responsible for the so-called homogeneous broadening.

(2) $\alpha \gg 1$ corresponds to the slow limit where the dynamics of the bath is slow compared to the inverse of the amplitude of the random frequency modulations. A Gaussian line shape $I(\omega) = \sqrt{\frac{2\pi}{\Omega^2}} e^{-\frac{\omega^2}{2\Omega^2}}$ is obtained in this case, characterized by a width Ω whose inhomogeneous character stems from the fact that each oscillator in an ensemble will experience different frequency shifts because of the slow dynamics of the environment, i.e., every oscillator will experience a “different” environment.

II. THEORY OF THE POLARITON LINE SHAPE

The Kubo-Anderson solution of the line shape of randomly modulated molecules treats a single molecule interacting with the radiation field and takes an average over an ensemble of such molecules. A naive extension to the molecule-in-cavity problem would be to consider an ensemble of systems, each comprising a single molecule and a cavity mode. However, such an extension is not relevant to many realistic experimental situations where the strong-coupling regime is achieved by employing many molecules collectively coupled to the cavity mode. By contrast, a physically sound extension of the Kubo-Anderson model consists of a cavity photon a_c coupled to N molecules a_j , essentially a Tavis-Cummings model [57] with modulated molecular transition frequencies. Note that the (static) disordered Tavis-Cummings model was recently investigated via the Green’s-function approach [30,36–38], and external environment effects on polaritonic response have also been studied [58,59]. Here we follow Anderson and Kubo and investigate both the static- and dynamic-disorder cases and the transition between them. We represent the molecules by classical harmonic oscillators [60] which, under driving by an incident radiation field $F e^{-i\omega t}$ [61], evolve

according to [62]

$$\begin{aligned} \dot{a}_c(t) &= -i\omega_c a_c - iu \sum_j a_j - \kappa a_c + iF e^{-i\omega t}, \\ \dot{a}_j(t) &= -i[\omega_m + \delta\omega_j(t)] a_j - iua_c - \gamma a_j, \end{aligned} \quad (2)$$

where ω_c is the photon frequency, ω_m is the time-independent molecular transition frequency, $\delta\omega_j(t)$ is the random frequency modulation of the molecular transition, u is the single-molecule coupling strength, and κ and γ are the dampings of the photon and molecules, respectively [63]. In the on-resonance case with $\omega_c = \omega_m$, the cavity response in the strong-coupling regime is characterized by two polariton peaks separated by the (collective) Rabi splitting $\Omega_R = 2\sqrt{N}u$. At steady state, the solutions oscillate with the driving frequency, i.e., $a_c(t) = \bar{a}_c(t) e^{-i\omega t}$ and $a_j(t) = \bar{a}_j(t) e^{-i\omega t}$, so the equations of motion become

$$\dot{\bar{a}}_c(t) = -i\bar{\omega}_c \bar{a}_c - iu \sum_j \bar{a}_j - \kappa \bar{a}_c + iF, \quad (3a)$$

$$\dot{\bar{a}}_j(t) = -i(\bar{\omega}_m + \delta\omega_j(t)) \bar{a}_j - iu \bar{a}_c - \gamma \bar{a}_j, \quad (3b)$$

where we have defined $\bar{\omega}_c \equiv \omega_c - \omega$ and $\bar{\omega}_m \equiv \omega_m - \omega$. The average total energy of the system $\langle E(t) \rangle = \omega_c \langle a_c^* a_c \rangle + \sum_j \omega_m \langle a_j^* a_j \rangle$ [64] satisfies, at steady state,

$$\left\langle \frac{dE}{dt} \right\rangle = \left\langle \frac{dE}{dt} \right\rangle_{\text{in}} + \left\langle \frac{dE}{dt} \right\rangle_{\text{out}} + \left\langle \frac{dE}{dt} \right\rangle_{\text{cav-mol}} = 0, \quad (4)$$

allowing us to identify the pumping and damping contributions as well as the energy exchange between the cavity and the molecules,

$$\left\langle \frac{dE}{dt} \right\rangle_{\text{in}} = i\omega_c (F \langle \bar{a}_c^* \rangle - F^* \langle \bar{a}_c \rangle), \quad (5a)$$

$$\left\langle \frac{dE}{dt} \right\rangle_{\text{out}} = -2\kappa \omega_c \langle |\bar{a}_c|^2 \rangle - 2\gamma \omega_m \sum_j \langle |\bar{a}_j|^2 \rangle, \quad (5b)$$

$$\left\langle \frac{dE}{dt} \right\rangle_{\text{cav-mol}} = iu \sum_j (\omega_c - \omega_m) (\langle \bar{a}_j^* \bar{a}_c \rangle - \langle \bar{a}_c^* \bar{a}_j \rangle). \quad (5c)$$

The absorption line shape may be obtained by evaluating

$$I(\omega) = i(F \langle \bar{a}_c^* \rangle - F^* \langle \bar{a}_c \rangle) \quad (6)$$

as a function of the incident frequency ω . To this end we need to find only $\langle \bar{a}_c \rangle$. For a single molecule outside the cavity, this approach leads to the familiar Kubo-Anderson result (see the Appendix for details).

We proceed by integrating Eq. (3b),

$$\begin{aligned} \bar{a}_j(t) &= \bar{a}_j(t_0) e^{-i\bar{\omega}_m(t-t_0) - \gamma(t-t_0) - i \int_{t_0}^t \delta\omega_j(t'') dt''} \\ &\quad - iu \int_{t_0}^t dt' e^{-i\bar{\omega}_m(t-t') - \gamma(t-t') - i \int_{t'}^t \delta\omega_j(t'') dt''} \bar{a}_c(t'), \end{aligned} \quad (7)$$

where the first term corresponds to the transient and only the second contributes to the steady-state solution. Using Eq. (7) in Eq. (3a), we find

$$\begin{aligned} \dot{\bar{a}}_c(t) = & -(i\bar{\omega}_c + \kappa)\bar{a}_c + iF \\ & - u^2 \sum_j^N \int_{-\infty}^t dt' e^{-i\bar{\omega}_m(t-t') - \gamma(t-t')} e^{-i \int_{t'}^t \delta\omega_j(t'') dt''} \bar{a}_c(t'). \end{aligned} \quad (8)$$

Also, at steady state (i.e., $t \rightarrow \infty$), $\bar{a}_c(t')$ can be taken outside the integral using the following argument: When t' is large (i.e., $t' \rightarrow t$), $\bar{a}_c(t')$ is a constant, while when t' is small (i.e.,

$t' \rightarrow -\infty$), the term vanishes. This leads to

$$\begin{aligned} \dot{\bar{a}}_c(t) = & -(i\bar{\omega}_c + \kappa)\bar{a}_c + iF \\ & - u^2 \bar{a}_c \int_{-\infty}^t dt' e^{-i\bar{\omega}_m(t-t') - \gamma(t-t')} \sum_j^N e^{-i \int_{t'}^t \delta\omega_j(t'') dt''}. \end{aligned} \quad (9)$$

Irrespective of the timescale of the frequency modulation,

$$\sum_j^N e^{-i \int_{t'}^t \delta\omega_j(t'') dt''} \approx N \langle e^{-i \int_{t'}^t \delta\omega_j(t'') dt''} \rangle \quad (10)$$

is a reasonable approximation for large N , leading to

$$\dot{\bar{a}}_c(t) = -(i\bar{\omega}_c + \kappa)\bar{a}_c + iF - Nu^2 \bar{a}_c \int_{-\infty}^t dt' e^{-i\bar{\omega}_m(t-t') - \gamma(t-t')} \langle e^{-i \int_{t'}^t \delta\omega_j(t'') dt''} \rangle, \quad (11)$$

and because at steady state $\langle \dot{\bar{a}}_c \rangle = 0$, it follows that

$$\langle \bar{a}_c \rangle = \frac{iF}{i\bar{\omega}_c + \kappa + Nu^2 \int_{-\infty}^t dt' e^{-i\bar{\omega}_m(t-t') - \gamma(t-t')} \langle e^{-i \int_{t'}^t \delta\omega_j(t'') dt''} \rangle}. \quad (12)$$

Knowing that $\langle e^{-i \int_{t'}^t \delta\omega_j(t'') dt''} \rangle$ is a function of $t - t'$ in the present model (see the Appendix), we have

$$\langle \bar{a}_c \rangle = \frac{iF}{i\bar{\omega}_c + \kappa + Nu^2 \int_0^\infty dt e^{-i\bar{\omega}_m t - \gamma t} \phi(t)}, \quad (13)$$

where the line-shape function $\phi(t)$ appears,

$$\phi(t) = \left\langle e^{i \int_0^t \delta\omega_j(t') dt'} \right\rangle, \quad (14)$$

a quantity well known in the Kubo-Anderson work [49,50,65]. Equation (13) will be our starting point to investigate the two limiting cases in which the molecular transition is either homogeneously or inhomogeneously broadened, as well as the intermediate regime.

As a final remark, note that in order to obtain a tractable expression such as Eq. (13) for both the fast and slow limits (see below), it was crucial to use Eq. (10) before taking ensemble averages. If we had otherwise set $\dot{\bar{a}}_c = 0$ in Eq. (9) for the slow case and taken the average over realizations, we would have obtained a far more complex expression for $\langle \bar{a}_c \rangle$ in the slow limit that would have required some approximation in order to be solved.

A. Fast limit

In the fast-modulation limit, one sets $\phi(t) = e^{-\Gamma t}$ [49,50]. Equation (13) then leads to

$$\langle \bar{a}_c \rangle = \frac{iF}{i\bar{\omega}_c + \kappa + \frac{Nu^2}{i\bar{\omega}_m + \gamma_m}}, \quad (15)$$

where $\gamma_m = \gamma + \Gamma$ is the total relaxation rate of the molecule, with pure dephasing rate Γ and lifetime broadening γ . From Eq. (6) we find the spectrum has a Lorentzian profile,

$$I(\omega) = |F|^2 \frac{2\kappa |i\bar{\omega}_m + \gamma_m|^2 + 2\gamma_m Nu^2}{|(i\bar{\omega}_c + \kappa)(i\bar{\omega}_m + \gamma_m) + Nu^2|^2}, \quad (16)$$

with the poles located at

$$\begin{aligned} \omega = & \frac{\omega_c + \omega_m - i(\gamma_m + \kappa)}{2} \\ & \pm \sqrt{Nu^2 + \left(\frac{\omega_c - \omega_m + i(\gamma_m - \kappa)}{2} \right)^2}. \end{aligned} \quad (17)$$

On resonance, we define $\omega_0 \equiv \omega_c = \omega_m$, and by assuming $\sqrt{Nu} \gg (\gamma_m - \kappa)/2$, which is reasonable since we are interested in the collective strong-coupling regime, we find the two polariton peaks at $\omega_0 \pm \sqrt{Nu} - \frac{i}{2}(\gamma_m + \kappa)$. These peaks are split by the collective Rabi splitting Ω_R , and each one inherits half of the original broadening of the cavity and molecular resonances. In particular when $\gamma_m = \kappa$, Eq. (16) becomes

$$I(\omega) = |F|^2 \left(\frac{\gamma_m}{(\bar{\omega}_0 - \sqrt{Nu})^2 + \gamma_m^2} + \frac{\gamma_m}{(\bar{\omega}_0 + \sqrt{Nu})^2 + \gamma_m^2} \right). \quad (18)$$

B. Slow limit

A shortcut to explore the effect of static disorder on polariton broadening is to use the fact that in the slow-modulation limit, $\delta\omega_j$ are time independent. Hence, $\dot{\bar{a}}_c = 0$, and $\dot{\bar{a}}_j = 0$, so from Eq. (3) for the on-resonance case we have

$$\bar{a}_c = \frac{iF}{i\bar{\omega}_0 + \kappa + \sum_j^N \frac{u^2}{i(\bar{\omega}_0 + \delta\omega_j) + \gamma}}, \quad (19)$$

and the line shape for a given realization [using Eq. (6) without the ensemble average] is

$$I(\omega) = |F|^2 \frac{2\kappa}{\left(\bar{\omega}_0 - \sum_j^N \frac{u^2}{\bar{\omega}_0 + \delta\omega_j} \right)^2 + \kappa^2}, \quad (20)$$

where for the sake of simplicity we have neglected homogeneous broadening ($\gamma = 0$). To make progress we expand the denominator for $\delta\omega_j/\bar{\omega}_0 \ll 1$ (which is satisfied in the vicinity of the polariton frequencies where $\bar{\omega}_0 \sim \pm\sqrt{N}u$ for strong enough coupling) and find

$$I(\omega) = |F|^2 \frac{2\kappa}{\left(\bar{\omega}_0 - \frac{Nu^2}{\bar{\omega}_0} + \frac{u^2}{\bar{\omega}_0^2} W_N\right)^2 + \kappa^2}, \quad (21)$$

where we have defined $W_N \equiv \sum_j^N \delta\omega_j$. This random number is characterized by the average $\langle W_N \rangle = 0$ and variance $\langle \delta W_N^2 \rangle = N \langle \delta\omega_j^2 \rangle$. To understand the effect of static disorder on the position and broadening of the peaks we must analyze the zeros of the following term:

$$\bar{\omega}_0 - \frac{Nu^2}{\bar{\omega}_0} + \frac{u^2}{\bar{\omega}_0^2} W_N = 0. \quad (22)$$

We proceed to solve the above expression for $\bar{\omega}_0 = \bar{\omega}_0^0 + \Delta\bar{\omega}_0$, where $\bar{\omega}_0^0 = \pm\sqrt{N}u$ and the effect of static disorder is contained in $\Delta\bar{\omega}_0$. To lowest order in $\Delta\bar{\omega}_0$ we find

$$\Delta\bar{\omega}_0 = -\frac{u^2}{2\bar{\omega}_0^0{}^2} W_N. \quad (23)$$

The variance of this term represents the effect that static disorder has on the broadening and is given by

$$\langle \delta\Delta\bar{\omega}_0^2 \rangle = \left(\frac{u^2}{2\bar{\omega}_0^0{}^2} \right)^2 \langle \delta W_N^2 \rangle \sim \frac{\langle \delta\omega_j^2 \rangle}{N}. \quad (24)$$

We see that $(\delta\Delta\bar{\omega}_0^2)^{1/2}$ scales like $1/\sqrt{N}$, confirming that in the collective regime, polaritons are immune to broadening due to static disorder for sufficiently large Rabi splitting. Note that the $1/\sqrt{N}$ scaling result was recently obtained with a more involved treatment [36].

A general expression for the line shape in the detuned case (i.e., without insisting that $\omega_m = \omega_c$) can be obtained using $\phi(t) = e^{-\frac{1}{2}\Omega^2 t^2}$ [49,50] (see the Appendix) in Eq. (13), leading to

$$\langle \bar{a}_c \rangle = \frac{iF}{i\bar{\omega}_c + \kappa + Nu^2 \sqrt{\frac{\pi}{2\Omega^2}} \left(1 - i\text{Erfi}\left[\frac{\bar{\omega}_m - i\gamma}{\sqrt{2\Omega^2}}\right] \right) e^{-\frac{(\bar{\omega}_m - i\gamma)^2}{2\Omega^2}}} \quad (25)$$

and

$$I(\omega) = |F|^2 \frac{2(\kappa + \tilde{\gamma})}{(\bar{\omega}_c + \Delta)^2 + (\kappa + \tilde{\gamma})^2}, \quad (26)$$

where $\tilde{\gamma}(\omega) \equiv Nu^2 \sqrt{\frac{\pi}{2\Omega^2}} e^{-\frac{\bar{\omega}_m^2}{2\Omega^2}}$ and $\Delta(\omega) \equiv -\tilde{\gamma} \text{Erfi}\left[\frac{\bar{\omega}_m}{\sqrt{2\Omega^2}}\right]$, with Erfi denoting the imaginary error function; for simplicity we have disregarded the intrinsic homogeneous broadening γ in the line-shape expression. This line shape is Lorentzian, and in addition to the cavity broadening κ there is one of molecular origin $\tilde{\gamma}$. Note that Eq. (26) is valid for any ratio of the Rabi splitting and inhomogeneous broadening Ω_R/Ω and therefore can describe the line shape of molecular polaritons for the important and common case that the inhomogeneous broadening of the molecular species is a considerable fraction of the Rabi splitting.

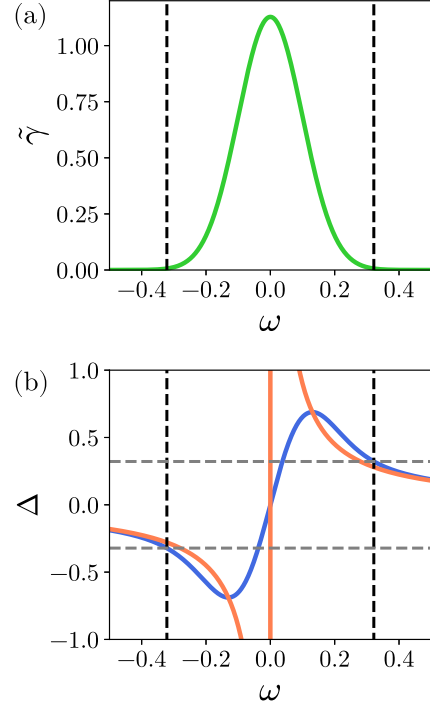


FIG. 1. (a) $\tilde{\gamma}$ and (b) Δ parameters as a function of the driving frequency. The blue line in (b) corresponds to the exact value, while the red line corresponds to the approximate one given in Eq. (27). The dashed black and gray lines indicate the polariton frequencies [poles of Eq. (26)]. The model parameters used here are $\omega_c = \omega_m = 0$, $\kappa = 0.02$, $\gamma = 0$, $\Omega = 0.1$, $\alpha = 50$, and $\Omega_R = 0.6$.

In Fig. 1 we plot $\tilde{\gamma}$ and Δ as a function of the driving frequency ω to gain some intuition on the significance of these parameters, with the dashed lines indicating the polariton frequencies. We do this for $\omega_c = \omega_m = 0$, $\kappa = 0.02$, $\alpha = 50$, $\Omega = 0.1$, and $\Omega_R = 0.6$. We see that $\tilde{\gamma}$ is a Gaussian function centered at ω_m with a variance of Ω , which is the amplitude of the frequency modulations. When the Rabi splitting is much larger than Ω , $\tilde{\gamma}$ does not contribute at the polariton frequencies, as easily seen in Fig. 1(a), and therefore, the width of the Lorentzian in Eq. (26) will be solely given by the cavity resonance broadening κ . Regarding the Δ parameter which determines the frequency of the poles of Eq. (26), as we can see in Fig. 1(b) (blue line), when the driving frequency coincides with the polariton frequencies (dashed vertical black lines), $\Delta(\omega)$ exactly corresponds to this value.

In Fig. 2 we plot analytical results for the spectrum in the slow-modulation limit, where we vary the relative size of the Rabi splitting with respect to the amplitude of the random frequency modulation Ω_R/Ω . We see that while outside the cavity the spectrum has a Gaussian profile, the polariton line shape in the strong-coupling regime is much narrower, with a Lorentzian line shape whose width is reduced as the Rabi splitting increases relative to the inhomogeneous broadening. Note that for $\Omega_R/\Omega \approx 2$ the two polariton peaks are already visible despite the Rabi splitting being only twice the inhomogeneous broadening. This is a common situation in molecular polaritons; for instance, in [66] the molecular band had a Gaussian-like profile with a FWHM ~ 530 meV,

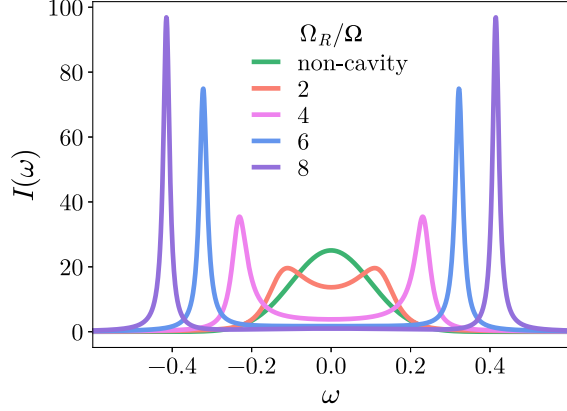


FIG. 2. Analytical spectrum for the slow-modulation limit in the non-cavity case [Eq. (A15)] and for the cavity case [Eq. (26)] for different ratios of the Rabi splitting divided by the amplitude of the random frequency modulation, Ω_R/Ω , where $\Omega_R = 2\sqrt{N}u$. The model parameters used here are $\omega_c = \omega_m = 0$, $\kappa = 0.02$, $\gamma = 0$, $\Omega = 0.1$, and $\alpha = 50$.

which corresponds to $\Omega \sim 300$ meV, and the Rabi splitting was ~ 600 meV. Also, note that for $\Omega_R/\Omega \approx 4$ (pink line) the narrowing in the line shape is already quite noticeable. We mention in passing that for small Ω_R/Ω , the two polariton bands arise from many eigenstates with a small cavity photon contribution and not two clean polaritons, as already extensively discussed in the literature [21,23,45,66].

We now further investigate the spectrum in Eq. (26) in the limit where the Rabi splitting is much larger than the amplitude of the frequency modulations. At the polariton frequencies, for small detuning, $\bar{\omega}_m \sim \pm\sqrt{N}u$, so by expanding Δ and $\tilde{\gamma}$ for $\sqrt{N}u/\sqrt{2}\Omega \gg 1$ we find that

$$\Delta(\omega) = -\frac{Nu^2}{\bar{\omega}_m} + O\left(\frac{1}{\sqrt{N}}\right) + i\tilde{\gamma} \quad (27)$$

and $\tilde{\gamma} \rightarrow 0$. Thus, in the limit when $\Omega_R/\Omega \gg 1$, $\tilde{\gamma}$ vanishes at the polariton frequencies, and only the cavity broadening remains. Note that the $1/\sqrt{N}$ scaling is in agreement with the result we obtained in Eq. (24). In Fig. 1(b) we plot this approximate Δ (red line) and verify that in the vicinity of the polariton frequencies, its value is very close to the exact one (blue line). Within this limit, the spectrum is then given by the following Lorentzian [which is consistent with Eq. (21)]:

$$I(\omega) = |F|^2 \frac{2\kappa}{\left(\bar{\omega}_c - \frac{Nu^2}{\bar{\omega}_m}\right)^2 + \kappa^2}. \quad (28)$$

In the strong-coupling regime ($\sqrt{N}u \gg \kappa/2$) and on resonance ($\omega_0 \equiv \omega_c = \omega_m$), the poles of this expression are located at $\omega \sim \omega_0 \pm \sqrt{N}u - i\kappa/2$ and $\omega \sim \omega_0 \pm \sqrt{N}u + i\kappa/2$ and correspond to the two polariton peaks. In Fig. 3 we plot the spectrum in Eq. (26) (solid lines) and compare it to the approximate one in Eq. (28) (dashed lines) for a series of parameters, where we increase the ratio of the Rabi splitting relative to the amplitude of the random frequency modulations. We observe that as Ω_R/Ω increases, both spectra converge.

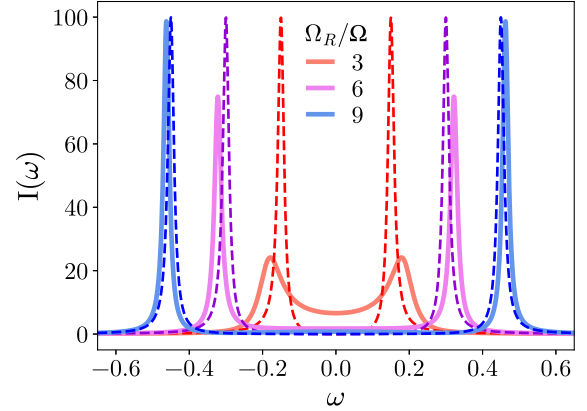


FIG. 3. Analytical spectrum for the slow-modulation limit calculated with Eq. (26) (solid lines) and Eq. (28) (dashed lines). Note that as the Rabi splitting increases relative to the inhomogeneous broadening, the approximate spectra converge to the exact ones. The model parameters used here are $\omega_c = \omega_m = 0$, $\kappa = 0.02$, $\Omega = 0.1$, and $\alpha = 50$.

C. Intermediate regime

We can also explore the intermediate regime where the correlation time of the random frequency modulations is comparable to the inverse of their amplitude, i.e., $\alpha \equiv \tau_c \Omega \approx 1$. To investigate the transition between the slow and fast limits we numerically calculate the spectrum with Eqs. (6) and (13). In this general case the ensemble-averaged quantity is given by [50,65] (see the Appendix)

$$\phi(t) = \exp\left[-\alpha^2\left(\frac{t}{\tau_c} - 1 + e^{-t/\tau_c}\right)\right], \quad (29)$$

with $\alpha \equiv \tau_c \Omega$ determining the transition between the fast ($\alpha \ll 1$) and slow ($\alpha \gg 1$) limits. In Fig. 4 we plot numerical results for varying parameter α , which controls the timescale of the frequency modulations relative to their amplitude. In all cases the spectrum smoothly transitions from the dynamic-to the static-disorder limit. For the two limits, $\alpha = 0.02$ and $\alpha = 50.0$, we plot (black dashed lines) the analytical spectrum which overlaps with the numerical results. While outside the cavity the line shape is very different in the fast and slow limits (Lorentzian vs Gaussian), such a difference is reduced inside the cavity as Ω_R/Ω increases. For instance, in Fig. 4(c), the line shape is fairly narrow regardless of α . Also, in these plots we can see that the frequency of the polariton peaks in the slow limit is slightly larger than that in the fast limit ($\pm 2\sqrt{N}u$), reflecting the effect of Δ in Eq. (26). Only when $\Omega_R \gg \Omega$ do the polariton frequencies for the slow limit coincide with those of the fast limit.

III. POLARITON LINEWIDTH

We further examine the effect of dynamic disorder and Rabi splitting on the polariton linewidth by fitting the polariton peak to either a Lorentzian,

$$I(\omega) = A_p \frac{\gamma_p}{(\omega - \omega_p)^2 + \gamma_p^2}, \quad (30)$$

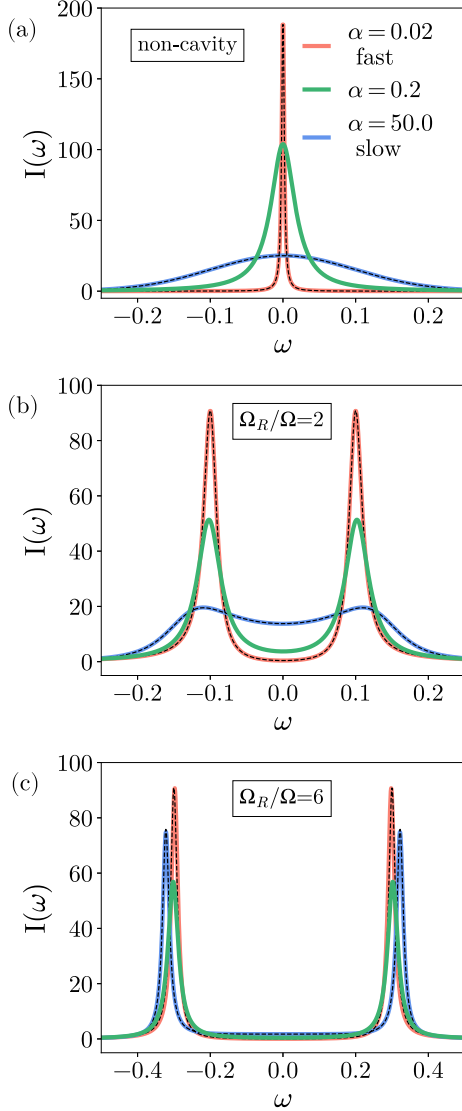


FIG. 4. Calculated spectrum for (a) the non-cavity case and cavity cases (b) $\Omega_R/\Omega = 2$ and (c) $\Omega_R/\Omega = 6$ for the fast- ($\alpha = 0.02$, red), intermediate- ($\alpha = 0.2$, green), and slow- ($\alpha = 50.0$, blue) modulation limits. The analytical spectrum for the fast and slow limits is also shown by black dashed lines, overlapping with the numerical results. Note that the non-cavity Lorentzian for the fast limit in (a) has been multiplied by a factor of 0.05. The model parameters used here are $\omega_c = \omega_m = 0$, $\kappa = 0.02$, $\gamma = 0$, and $\Omega = 0.1$.

or a Voigt profile,

$$I(\omega) = A_p \sqrt{\frac{2\pi}{\sigma_p^2}} \Re[W(z)], \quad z = \frac{(\omega - \omega_p + i\gamma_p)}{\sqrt{2\sigma_p^2}}, \quad (31)$$

where ω_p is the central position of the peak, A_p is an amplitude, $W(z) = e^{-z^2} \text{Erfc}[-iz]$ is the Faddeeva function, and Erfc denotes the complementary error function. Note that when fitting our data to a Voigt profile, we extract two parameters (γ_p and ω_p), both of which are reported below.

In Fig. 5 we show the polariton linewidth as a function of Ω_R/Ω . Note that since we are considering the zero-detuned

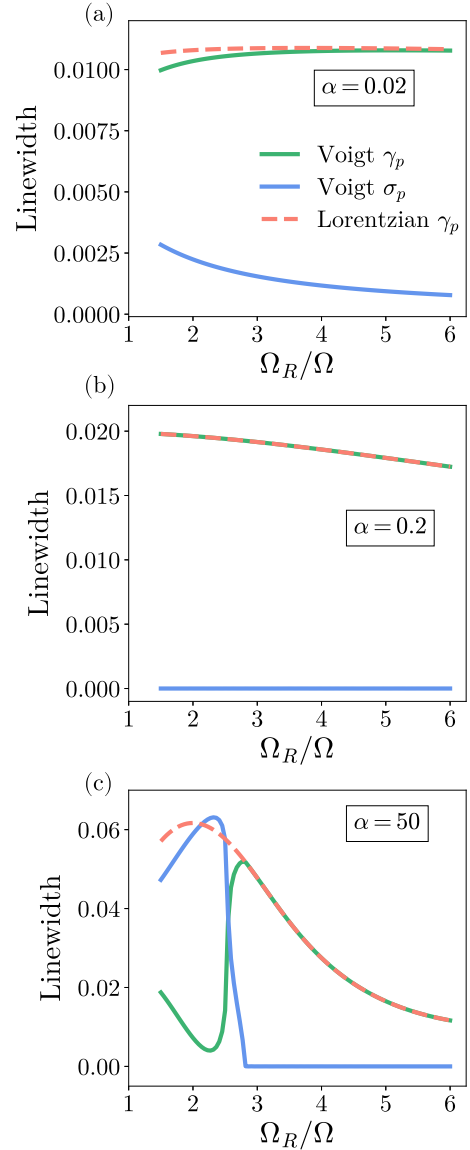


FIG. 5. Polariton linewidth as a function of Ω_R/Ω for (a) fast-, (b) intermediate-, and (c) slow-disorder cases. Linewidth extracted from fitting to either a Lorentzian profile [Eq. (30)] or Voigt profile [Eq. (31)]. The model parameters used here are $\omega_c = \omega_m = 0$, $\kappa = 0.02$, $\gamma = 0$, and $\Omega = 0.1$.

case, both polaritons are equally broadened. For the fast-disorder case ($\alpha = 0.02$), the linewidth is Lorentzian, as expected. For the intermediate-disorder case ($\alpha = 0.2$), the linewidth is also Lorentzian and is slightly reduced as Ω_R/Ω increases. For the slow-disorder case ($\alpha = 50$), polariton narrowing for increased Rabi splitting is more evident, where one can clearly see a crossover between a Gaussian and a Lorentzian broadening.

In Fig. 6 we plot the polariton linewidth as a function of α for the $\Omega_R/\Omega = 2$ case shown in Fig. 4(b). While for $\alpha \lesssim 1$, i.e., the fast- and intermediate-disorder cases, the linewidth is Lorentzian, for $\alpha \gg 1$, i.e., the static-disorder limit, the linewidth is Gaussian.

In Fig. 7 we explore the effect of detuning on the lower polariton linewidth for the slow-disorder case. The different

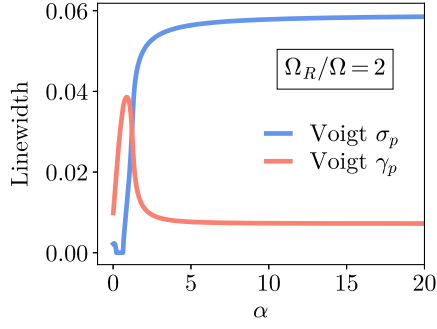


FIG. 6. Polariton linewidth as a function of α for $\Omega_R/\Omega = 2$. Linewidth extracted from fitting to a Voigt profile [Eq. (31)]. The model parameters used here are $\omega_c = \omega_m = 0$, $\kappa = 0.02$, $\gamma = 0$, and $\Omega = 0.1$.

shapes of the curves reflect the fact that the lower polariton evolves from more photon-like to more molecule dominated as the detuning $\Delta = \omega_c - \omega_m$ increases. Note that similar plots were reported in the past for exciton polaritons in semiconductor microcavities [8,9] and very recently for molecular polaritons [44].

IV. CONCLUSIONS

We extended Kubo-Anderson's theory of the stochastic line shape to a model problem of coupled, driven, and damped (classical) harmonic oscillators describing polaritons formed in the strong-coupling regime. We derived analytic expressions for the polariton line shape in the limits of fast and slow

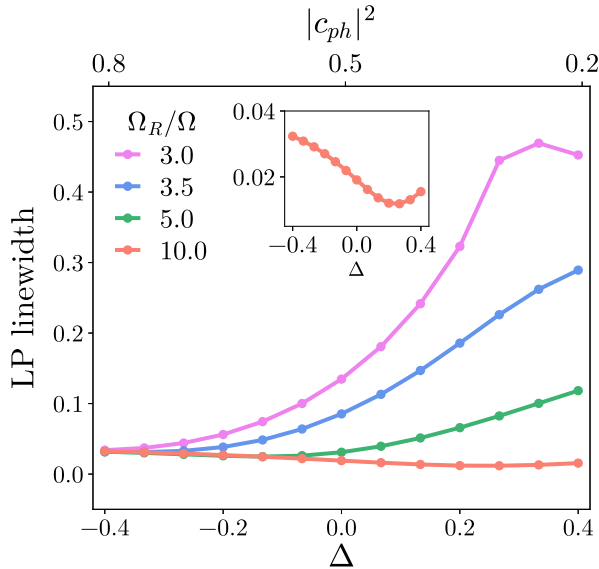


FIG. 7. The linewidth of the lower polariton (LP) as a function of detuning, $\Delta = \omega_c - \omega_m$, for different Ω_R/Ω . The photonic weight (Hopfield coefficient) is calculated for the LP in the case of a nondisordered Tavis-Cummings model. The linewidth corresponds to the half width at half maximum extracted from the spectra. The model parameters used here are $\omega_c = 0$, $\kappa = 0.02$, $\gamma = 0$, $\Omega_R = 0.5$, and $\alpha = 50$. The inset zooms into the data points for the $\Omega_R/\Omega = 10$ case.

disorder of the molecular transition frequency and numerically explored the intermediate regime as well. Our theory predicts that polaritons inherit half the original homogeneous broadening of the cavity and molecular resonance, while static disorder does not contribute to their broadening for large enough Rabi splitting, in agreement with experimental observations and previous numerical calculations. Our results also provide an analytical expression for the polariton line shape valid for any degree of static disorder relative to the Rabi splitting, which is especially relevant within the context of molecular polaritons, in which the inhomogeneous broadening of the molecular transition can be a significant fraction of the Rabi splitting.

ACKNOWLEDGMENTS

C.C. thanks the Vagelos Institute for Energy, Science, and Technology (VIEST) for a postdoctoral fellowship that initially supported this work. This project received funding from the European Union's Horizon 2020 Research and Innovation Programme under Marie Skłodowska-Curie Grant Agreement No. 101029374. This work was supported by the U.S. Department of Energy, Office of Science, Office of Basic Energy Sciences, under Award No. DE-SC0019397 (J.E.S.). The research of A.N. is supported by the Air Force Office of Scientific Research under Award No. FA9550-23-1-0368 and the University of Pennsylvania.

APPENDIX: RETRIEVING THE ORIGINAL KUBO-ANDERSON RESULT

In the original Kubo-Anderson model, the line shape of the randomly modulated oscillator in Eq. (1) was obtained by calculating the Fourier transform of the autocorrelation function of the amplitude a [51]. The physical justification behind this approach is that the Wiener-Khinchine theorem states that the spectral decomposition of the autocorrelation function of a random stationary process corresponds to its power spectrum. Also, the position of the oscillator is $x \sim (a + a^*)$, and so at thermal equilibrium, $\langle x(0)x(t) \rangle \sim \langle a^*(0)a(t) \rangle$ [65].

In the main text we used a different approach to extend the Kubo-Anderson theory to the case of the polariton line shape. In particular, we obtained the spectral response by calculating the steady state of a collection of coupled, driven, and damped harmonic oscillators. In the following we show that this approach reduces to the original Kubo result for the case of a single molecule. The equation of motion for a driven and damped oscillator with a randomly modulated frequency is

$$\dot{a}(t) = -i[\omega_0 + \delta\omega(t)]a - \gamma a + iF e^{-i\omega t}, \quad (\text{A1})$$

where we now drop the j index for the molecule. We are looking for the steady state, where the solutions will oscillate with the driving frequency. By setting $\bar{a} = a e^{-i\omega t}$ and $\bar{\omega}_0 \equiv \omega_0 - \omega$, the equation of motion reads

$$\dot{\bar{a}}(t) = -i[\bar{\omega}_0 + \delta\omega(t)]\bar{a} - \gamma \bar{a} + iF. \quad (\text{A2})$$

In the steady state, the average energy is constant with time, $\langle \frac{dE}{dt} \rangle = 0$, yielding

$$-2\gamma \langle |\bar{a}|^2 \rangle + i(F \langle \bar{a}^* \rangle - F^* \langle \bar{a} \rangle) = 0, \quad (\text{A3})$$

and so the absorption spectrum may be calculated by evaluating the first term, which corresponds to the damping contribution, or the last two terms, which correspond to the driving energy input.

The solution to the differential equation in Eq. (A2) is given by

$$\begin{aligned} \bar{a}(t) = & \bar{a}(t_0) e^{-i\bar{\omega}_0(t-t_0) - \gamma(t-t_0) - i \int_{t_0}^t \delta\omega(t') dt'} \\ & + iF \int_{t_0}^t dt' e^{-i\bar{\omega}_0(t-t') - \gamma(t-t') - i \int_{t_0}^{t'} \delta\omega(t'') dt''}. \end{aligned} \quad (\text{A4})$$

We are interested in the long-time dynamics, the stationary state. By taking $t_0 = -\infty$, the first term does not contribute, and the solution is given by the second term. Hence,

$$\langle \bar{a} \rangle = iF \int_{t_0}^t dt' e^{-i\bar{\omega}_0(t-t') - \gamma(t-t')} \phi(t, t'), \quad (\text{A5})$$

where

$$\phi(t, t') \equiv \left\langle e^{-i \int_{t'}^t \delta\omega(t'') dt''} \right\rangle. \quad (\text{A6})$$

This average quantity may be calculated from cumulant averages as in [67],

$$\phi(t, t') = e^{-\frac{i}{2} \int_{t'}^t dt_1 \int_{t'}^{t_1} dt_2 \langle \delta\omega(t_1) \delta\omega(t_2) \rangle}. \quad (\text{A7})$$

For the standard Kubo-Anderson model we assume that $\langle \delta\omega(t) \delta\omega(t + \tau) \rangle = \Omega^2 s(\tau)$, where $\Omega = \sqrt{\langle \delta\omega^2 \rangle}$ and $s(\tau) = s(-\tau)$. After some manipulation of the integral (as in [65]) one can show that

$$\phi(t, t') = e^{-\Omega^2 \int_0^{\tilde{t}} d\tau s(\tau) (\tilde{t} - \tau)}, \quad (\text{A8})$$

where $\tilde{t} = t - t'$. Taking $s(\tau) = e^{-\tau/\tau_c}$ [52], we obtain

$$\phi(\tilde{t}) = \exp \left[-\alpha^2 \left(\frac{\tilde{t}}{\tau_c} - 1 + e^{-\tilde{t}/\tau_c} \right) \right] \quad (\text{A9})$$

which is a function of $t - t'$. After a change of variables in Eq. (A5) we find

$$\langle \bar{a} \rangle = iF \int_0^\infty dt e^{-i\bar{\omega}_0 t - \gamma t} \phi(t), \quad (\text{A10})$$

where

$$\phi(t) = \left\langle e^{i \int_0^t \delta\omega(t') dt'} \right\rangle. \quad (\text{A11})$$

The fast ($\alpha \ll 1$) and slow ($\alpha \gg 1$) limits of the Kubo-Anderson model from Eq. (A9) result in

$$\phi(t) = \begin{cases} e^{-\Gamma t}, & \text{fast limit, } \Gamma = \tau_c \Omega^2, \\ e^{-\frac{1}{2} \Omega^2 t^2}, & \text{slow limit.} \end{cases} \quad (\text{A12})$$

The spectrum may now be calculated analytically with the last two terms in Eq. (A3) together with Eq. (A10).

In the fast limit, the spectrum is given by

$$\begin{aligned} I(\omega) = & |F|^2 \left(\int_0^\infty dt e^{i\bar{\omega}_0 t - \gamma t} e^{-\Gamma t} + \int_0^\infty dt e^{-i\bar{\omega}_0 t - \gamma t} e^{-\Gamma t} \right) \\ = & |F|^2 \frac{2(\gamma + \Gamma)}{\bar{\omega}_0^2 + (\gamma + \Gamma)^2}, \end{aligned} \quad (\text{A13})$$

which reduces to the Kubo-Anderson result (when $\gamma = 0$): a Lorentzian line shape with width Γ representing the case of homogeneous broadening (due to pure dephasing). In the slow limit the spectrum is given by

$$\begin{aligned} I(\omega) = & |F|^2 \left(\int_0^\infty dt e^{i\bar{\omega}_0 t - \gamma t} e^{-\frac{1}{2} \Omega^2 t^2} \right. \\ & \left. + \int_0^\infty dt e^{-i\bar{\omega}_0 t - \gamma t} e^{-\frac{1}{2} \Omega^2 t^2} \right) \\ = & \frac{1}{2} |F|^2 \sqrt{\frac{2\pi}{\Omega^2}} \left(\text{Erfc} \left[\frac{(-i\bar{\omega}_0 + \gamma)}{\sqrt{2\Omega^2}} \right] e^{\frac{1}{2\Omega^2} (-i\bar{\omega}_0 + \gamma)^2} \right. \\ & \left. + \text{Erfc} \left[\frac{(i\bar{\omega}_0 + \gamma)}{\sqrt{2\Omega^2}} \right] e^{\frac{1}{2\Omega^2} (i\bar{\omega}_0 + \gamma)^2} \right), \end{aligned} \quad (\text{A14})$$

where Erfc is the complementary error function. By setting $\gamma = 0$ we recover the Kubo-Anderson result of a Gaussian line shape representing the case of inhomogeneous broadening:

$$I(\omega) = |F|^2 \sqrt{\frac{2\pi}{\Omega^2}} e^{-\frac{\omega_0^2}{2\Omega^2}}. \quad (\text{A15})$$

-
- [1] A. V. Kavokin, J. J. Baumberg, G. Malpuech, and F. P. Laussy, *Microcavities* (Oxford University Press, Oxford, 2007).
[2] T. E. Li, B. Cui, J. E. Subotnik, and A. Nitzan, Molecular polaritonics: Chemical dynamics under strong light-matter coupling, *Annu. Rev. Phys. Chem.* **73**, 43 (2022).
[3] S. Pau, G. Björk, J. Jacobson, H. Cao, and Y. Yamamoto, Microcavity exciton-polariton splitting in the linear regime, *Phys. Rev. B* **51**, 14437 (1995).
[4] R. Houdré, R. P. Stanley, and M. Illegems, Vacuum-field Rabi splitting in the presence of inhomogeneous broadening: Resolution of a homogeneous linewidth in an inhomogeneously broadened system, *Phys. Rev. A* **53**, 2711 (1996).
[5] C. Ell, J. Prineas, T. R. Nelson, S. Park, H. M. Gibbs, G. Khitrova, S. W. Koch, and R. Houdré, Influence of

structural disorder and light coupling on the excitonic response of semiconductor microcavities, *Phys. Rev. Lett.* **80**, 4795 (1998).

- [6] J. P. Long and B. S. Simpkins, Coherent coupling between a molecular vibration and Fabry-Perot optical cavity to give hybridized states in the strong coupling limit, *ACS Photonics* **2**, 130 (2015).
[7] V. Savona and C. Weisbuch, Theory of time-resolved light emission from polaritons in a semiconductor microcavity under resonant excitation, *Phys. Rev. B* **54**, 10835 (1996).
[8] P. Kinsler and D. M. Whittaker, Linewidth narrowing of polaritons, *Phys. Rev. B* **54**, 4988 (1996).
[9] D. M. Whittaker, P. Kinsler, T. A. Fisher, M. S. Skolnick, A. Armitage, A. M. Afshar, M. D. Sturge, and J. S. Roberts,

- Motional narrowing in semiconductor microcavities, *Phys. Rev. Lett.* **77**, 4792 (1996).
- [10] S. Pau, G. Björk, H. Cao, E. Hanamura, and Y. Yamamoto, Theory of inhomogeneous microcavity polariton splitting, *Solid State Commun.* **98**, 781 (1996).
- [11] V. Savona and C. Piermarocchi, Microcavity polaritons: Homogeneous and inhomogeneous broadening in the strong coupling regime, *Phys. Status Solidi A* **164**, 45 (1997).
- [12] V. Savona, C. Piermarocchi, A. Quattropani, F. Tassone, and P. Schwendimann, Microscopic theory of motional narrowing of microcavity polaritons in a disordered potential, *Phys. Rev. Lett.* **78**, 4470 (1997).
- [13] A. V. Kavokin, Motional narrowing of inhomogeneously broadened excitons in a semiconductor microcavity: Semiclassical treatment, *Phys. Rev. B* **57**, 3757 (1998).
- [14] L. C. Andreani, G. Panzarini, A. V. Kavokin, and M. R. Vladimirova, Effect of inhomogeneous broadening on optical properties of excitons in quantum wells, *Phys. Rev. B* **57**, 4670 (1998).
- [15] D. M. Whittaker, What determines inhomogeneous linewidths in semiconductor microcavities? *Phys. Rev. Lett.* **80**, 4791 (1998).
- [16] P. Borri, W. Langbein, U. Woggon, J. R. Jensen, and J. M. Hvam, Microcavity polariton linewidths in the weak-disorder regime, *Phys. Rev. B* **63**, 035307 (2000).
- [17] M. Litinskaia, G. C. La Rocca, and V. M. Agranovich, Inhomogeneous broadening of polaritons in high-quality microcavities and weak localization, *Phys. Rev. B* **64**, 165316 (2001).
- [18] V. M. Agranovich, M. Litinskaia, and D. G. Lidzey, Cavity polaritons in microcavities containing disordered organic semiconductors, *Phys. Rev. B* **67**, 085311 (2003).
- [19] F. M. Marchetti, J. Keeling, M. H. Szymańska, and P. B. Littlewood, Thermodynamics and excitations of condensed polaritons in disordered microcavities, *Phys. Rev. Lett.* **96**, 066405 (2006).
- [20] J.-M. Manceau, G. Biasiol, N. L. Tran, I. Carusotto, and R. Colombelli, Immunity of intersubband polaritons to inhomogeneous broadening, *Phys. Rev. B* **96**, 235301 (2017).
- [21] P. Michetti and G. C. La Rocca, Polariton states in disordered organic microcavities, *Phys. Rev. B* **71**, 115320 (2005).
- [22] P. Michetti and G. C. La Rocca, Polariton dynamics in disordered microcavities, *Phys. E* **40**, 1926 (2008).
- [23] P. Michetti, L. Mazza, and G. C. La Rocca, Strongly coupled organic microcavities, in *Organic Nanophotonics: Fundamentals and Applications*, edited by Y. S. Zhao (Springer, Berlin, 2015), pp. 39–68.
- [24] J. Feist and F. J. Garcia-Vidal, Extraordinary exciton conductance induced by strong coupling, *Phys. Rev. Lett.* **114**, 196402 (2015).
- [25] G. D. Scholes, Polaritons and excitons: Hamiltonian design for enhanced coherence, *Proc. R. Soc. A* **476**, 20200278 (2020).
- [26] C. Sommer, M. Reitz, F. Mineo, and C. Genes, Molecular polaritonics in dense mesoscopic disordered ensembles, *Phys. Rev. Res.* **3**, 033141 (2021).
- [27] D. Wellnitz, G. Pupillo, and J. Schachenmayer, Disorder enhanced vibrational entanglement and dynamics in polaritonic chemistry, *Commun. Phys.* **5**, 120 (2022).
- [28] B. Cohn, S. Sufrin, A. Basu, and L. Chuntonov, Vibrational polaritons in disordered molecular ensembles, *J. Phys. Chem. Lett.* **13**, 8369 (2022).
- [29] G. Engelhardt and J. Cao, Unusual dynamical properties of disordered polaritons in microcavities, *Phys. Rev. B* **105**, 064205 (2022).
- [30] G. Engelhardt and J. Cao, Polariton localization and dispersion properties of disordered quantum emitters in multimode microcavities, *Phys. Rev. Lett.* **130**, 213602 (2023).
- [31] E. Suyabatmaz and R. F. Ribeiro, Vibrational polariton transport in disordered media, *J. Chem. Phys.* **159**, 034701 (2023).
- [32] F. Herrera and M. Litinskaya, Disordered ensembles of strongly coupled single-molecule plasmonic picocavities as nonlinear optical metamaterials, *J. Chem. Phys.* **156**, 114702 (2022).
- [33] T. F. Allard and G. Weick, Disorder-enhanced transport in a chain of lossy dipoles strongly coupled to cavity photons, *Phys. Rev. B* **106**, 245424 (2022).
- [34] J. B. Pérez-Sánchez, F. Mellini, J. Yuen-Zhou, and N. C. Giebink, Collective polaritonic effects on chemical dynamics suppressed by disorder, *Phys. Rev. Res.* **6**, 013222 (2024).
- [35] K. Schwennicke, N. C. Giebink, and J. Yuen-Zhou, Extracting accurate light-matter couplings from disordered polaritons, *Nanophotonics* (2024).
- [36] T. Gera and K. L. Sebastian, Effects of disorder on polaritonic and dark states in a cavity using the disordered Tavis–Cummings model, *J. Chem. Phys.* **156**, 194304 (2022).
- [37] T. Gera and K. L. Sebastian, Exact results for the Tavis–Cummings and Hückel Hamiltonians with diagonal disorder, *J. Phys. Chem. A* **126**, 5449 (2022).
- [38] M. A. Zeb, Analytical solution of the disordered Tavis–Cummings model and its Fano resonances, *Phys. Rev. A* **106**, 063720 (2022).
- [39] H.-T. Chen, Z. Zhou, M. Sukharev, J. E. Subotnik, and A. Nitzan, Interplay between disorder and collective coherent response: Superradiance and spectral motional narrowing in the time domain, *Phys. Rev. A* **106**, 053703 (2022).
- [40] Z. Zhou, H.-T. Chen, J. E. Subotnik, and A. Nitzan, Interplay between disorder, local relaxation, and collective behavior for an ensemble of emitters outside versus inside a cavity, *Phys. Rev. A* **108**, 023708 (2023).
- [41] R. Pandya, A. Ashoka, K. Georgiou, J. Sung, R. Jayaprakash, S. Renken, L. Gai, Z. Shen, A. Rao, and A. J. Musser, Tuning the coherent propagation of organic exciton-polaritons through dark state delocalization, *Adv. Sci.* **9**, 2105569 (2022).
- [42] A. George, T. Geraghty, Z. Kelsey, S. Mukherjee, G. Davidova, W. Kim, and A. J. Musser, Controlling the manifold of polariton states through molecular disorder, *Adv. Opt. Mater.* **12**, 2302387 (2024).
- [43] S. Gunasekaran, R. F. Pinard, and A. J. Musser, Continuum model of strong light-matter coupling for molecular polaritons, [arXiv:2308.08744](https://arxiv.org/abs/2308.08744).
- [44] S. T. Wanasinghe, A. Gjoni, W. Burson, C. Majeski, B. Zaslona, and A. S. Rury, Motional narrowing through photonic exchange: Rational suppression of excitonic disorder from molecular cavity polariton formation, *J. Phys. Chem. Lett.* **15**, 2405 (2024).
- [45] G. Groenhof, C. Climent, J. Feist, D. Morozov, and J. J. Toppari, Tracking polariton relaxation with multiscale molecular dynamics simulations, *J. Phys. Chem. Lett.* **10**, 5476 (2019).

- [46] C. Climent, D. Casanova, J. Feist, and F. J. Garcia-Vidal, Not dark yet for strong light-matter coupling to accelerate singlet fission dynamics, *Cell Rep. Phys. Sci.* **3**, 100841 (2022).
- [47] N. Bradbury, R. Ribeiro, J. R. Caram, and D. Neuhauser, Polaritons in large stochastic simulations of 2D molecular aggregates, [arXiv:2308.04385](https://arxiv.org/abs/2308.04385).
- [48] P. W. Anderson and P. R. Weiss, Exchange narrowing in paramagnetic resonance, *Rev. Mod. Phys.* **25**, 269 (1953).
- [49] P. W. Anderson, A mathematical model for the narrowing of spectral lines by exchange or motion, *J. Phys. Soc. Jpn.* **9**, 316 (1954).
- [50] R. Kubo, Note on the stochastic theory of resonance absorption, *J. Phys. Soc. Jpn.* **9**, 935 (1954).
- [51] R. Kubo, Stochastic theory of magnetic resonance, *Nuovo Cimento* **6**, 1063 (1957).
- [52] R. Kubo, Stochastic Liouville equations, *J. Math. Phys.* **4**, 174 (1963).
- [53] R. Kubo, A stochastic theory of line shape, in *Advances in Chemical Physics* (Wiley, New York, 1969), pp. 101–127.
- [54] N. Bloembergen, E. M. Purcell, and R. V. Pound, Relaxation effects in nuclear magnetic resonance absorption, *Phys. Rev.* **73**, 679 (1948).
- [55] C. P. Slichter, *Principles of Magnetic Resonance*, Springer Series in Solid-State Sciences (Springer, Berlin, 1996).
- [56] Note that the term “motional narrowing” has led to misleading interpretations in the past when describing narrowing of the polariton linewidth in semiconductor microcavities [9,12,13]. Static disorder (and not fast disorder) appears to be responsible for such narrowing [4,5].
- [57] M. Tavis and F. W. Cummings, Exact solution for an N -molecule-radiation-field Hamiltonian, *Phys. Rev.* **170**, 379 (1968).
- [58] K. S. U. Kansanen, J. J. Toppari, and T. T. Heikkilä, Polariton response in the presence of Brownian dissipation from molecular vibrations, *J. Chem. Phys.* **154**, 044108 (2021).
- [59] M. Harder, L. Bai, C. Match, J. Sirker, and C. Hu, Study of the cavity-magnon-polariton transmission line shape *Sci. China: Phys., Mech. Astron.* **59**, 117511 (2016).
- [60] Note that under weak driving, we do not expect differences between the classical and quantum descriptions given that a classical damped harmonic oscillator reproduces the same physics as the Bloch equations of a two-level system.
- [61] We take $F = 1$ in the calculations.
- [62] In addressing the driven Tavis-Cummings model one may choose to couple the molecules or the cavity mode to the external radiation field, and we take the latter as a more physically appealing choice. If one were to solve the original out-of-cavity Kubo-Anderson problem with this approach, the driving would obviously be on the molecule, $\dot{a}_j(t) = -i[\omega_m + \delta\omega_j(t)]a_j - \gamma a_j + iF e^{-i\omega t}$.
- [63] The relaxation parameter γ is needed to facilitate the steady-state treatment that follows. It may be set to zero at the end of the calculation or kept to reflect the finite lifetime of individual molecules. Collective (superradiant) relaxation (see, e.g., [39,40]) is disregarded in the present treatment.
- [64] We have not included the $\delta\omega_j(t)$ contribution to the energy because these fluctuations are much smaller than ω_m .
- [65] A. Nitzan, *Chemical Dynamics in Condensed Phases: Relaxation, Transfer and Reactions in Condensed Molecular Systems* (Oxford University Press, Oxford, 2006).
- [66] J. Mony, C. Climent, A. U. Petersen, K. Moth-Poulsen, J. Feist, and K. Börjesson, Photoisomerization efficiency of a solar thermal fuel in the strong coupling regime, *Adv. Funct. Mater.* **31**, 2010737 (2021).
- [67] R. Kubo, Generalized cumulant expansion method, *J. Phys. Soc. Jpn.* **17**, 1100 (1962).